

Nucleation of ordered solid phases of proteins via a disordered high-density state: Phenomenological approach

Cite as: J. Chem. Phys. **122**, 174905 (2005); <https://doi.org/10.1063/1.1887168>

Submitted: 28 September 2004 • Accepted: 15 February 2005 • Published Online: 04 May 2005

Weichun Pan, Anatoly B. Kolomeisky and Peter G. Vekilov



View Online



Export Citation

ARTICLES YOU MAY BE INTERESTED IN

[Kinetics of two-step nucleation of crystals](#)

The Journal of Chemical Physics **122**, 244706 (2005); <https://doi.org/10.1063/1.1943389>

[Spinodal for the solution-to-crystal phase transformation](#)

The Journal of Chemical Physics **123**, 014904 (2005); <https://doi.org/10.1063/1.1943413>

[Crystal nucleation in the presence of a metastable critical point](#)

The Journal of Chemical Physics **109**, 223 (1998); <https://doi.org/10.1063/1.476554>

[Learn More](#)

The Journal of Chemical Physics **Special Topics** Open for Submissions

Nucleation of ordered solid phases of proteins via a disordered high-density state: Phenomenological approach

Weichun Pan

Department of Chemical Engineering, University of Houston, Houston, Texas 77204-4004

Anatoly B. Kolomeisky

Department of Chemistry, Rice University, Houston, Texas 77005-1892

Peter G. Vekilov

Department of Chemical Engineering, University of Houston, Houston, Texas 77204-4004

(Received 28 September 2004; accepted 15 February 2005; published online 4 May 2005)

Nucleation of ordered solid phases of proteins triggers numerous phenomena in laboratory, industry, and in healthy and sick organisms. Recent simulations and experiments with protein crystals suggest that the formation of an ordered crystalline nucleus is preceded by a disordered high-density cluster, akin to a droplet of high-density liquid that has been observed with some proteins; this mechanism allowed a qualitative explanation of recorded complex nucleation kinetics curves. Here, we present a simple phenomenological theory that takes into account intermediate high-density metastable states in the nucleation process. Nucleation rate data at varying temperature and protein concentration are reproduced with high fidelity using literature values of the thermodynamic and kinetic parameters of the system. Our calculations show that the growth rate of the near-critical and supercritical ordered clusters within the dense intermediate is a major factor for the overall nucleation rate. This highlights the role of viscosity within the dense intermediate for the formation of the ordered nucleus. The model provides an understanding of the action of additives that delay or accelerate nucleation and presents a framework within which the nucleation of other ordered protein solid phases, e.g., the sickle cell hemoglobin polymers, can be analyzed. © 2005 American Institute of Physics. [DOI: 10.1063/1.1887168]

I. INTRODUCTION

The formation of protein ordered phases is of interest to many scientific and technological areas: structural biology,¹⁻³ patho-physiology of protein condensation diseases,⁴⁻⁶ production of protein pharmaceutical preparations,^{7,8} etc., and a deeper understanding of the underlying mechanisms is expected to facilitate progress in these areas.

The phase diagrams of protein solutions differ from those of simple substances, such as argon. The significant factor underlying this difference is the range of attraction between molecules:⁹⁻¹¹ this range is determined by the size of the solvent molecules¹² (at the typically used ionic strengths of ≥ 0.1 M the electrostatics is screened and the Deriaguine-Landau-Veevey-Overback theory does not apply^{13,14}), smaller by at least an order of magnitude than the protein molecules' sizes. As a result, in protein solutions the triple point disappears and the liquid-liquid (*L-L*) phase separation is submerged below the solution-crystal equilibrium.^{15,16} Phase diagrams with a *L-L* separation line with a critical point lying below a smooth liquidus and a solidus lines have been found for several proteins.¹⁷⁻²¹

An investigation of the crystal nucleation mechanisms using the protein lysozyme revealed an unusual dependence of the rate of homogeneous nucleation on temperature: as the temperature is lowered from the equilibrium, the dependence passes through a maximum in the vicinity of liquid-liquid phase boundary,²² Fig. 1. Another unusual result with the

same system was that as supersaturation is increased, the nucleus size decreases and reaches one molecule.²³ This transition occurs at conditions that differ by 1.0 °C– 1.5 °C (or ~ 10 – 15 mg ml⁻¹) from the *L-L* coexistence line in the (temperature, protein concentration) plane and indicates that the nucleation free-energy barrier becomes less than the thermal energy and the rate of nucleation is solely limited by the kinetics of growth of the near-critical clusters.²⁴⁻²⁶ These two observations contradict the assumptions and predictions of the classical nucleation theory.²⁷

Prompted by computer simulations²⁸ and density functional calculations²⁹ results in the vicinity of the *L-L* critical point, the above unusual behavior of the nucleation rate was explained by the presence of a dense liquid intermediate in the nucleation reaction pathway, Fig. 2.^{22,30} Since the nucleation rate maximum is consistently reached above the *L-L* coexistence line, it was concluded that a dense-liquid-like droplet, unstable or metastable with respect to the low density solution, serves as an intermediate in that region, Fig. 2.³⁰ Similar interpretations of these results were offered in several theoretical and computational investigations of protein crystallization.³¹⁻³³ Note also that the protein nucleation is a complex phenomenon that cannot be described by a single order parameter. Thus Fig. 2 is a simplified formal presentation of a free-energy landscape of the system, and the nucleation reaction coordinate might include several order parameters.

In this paper we develop a simple phenomenological

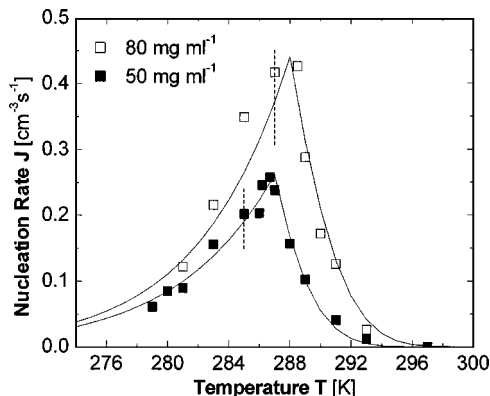


FIG. 1. The dependence of the rate of homogeneous nucleation J of lysozyme crystals on temperature T at two fixed lysozyme concentration indicated in the plot. The temperatures of equilibrium between crystals and solution are 315 K at $C_{\text{lys}}=50 \text{ mg ml}^{-1}$ and 319 K at $C_{\text{lys}}=80 \text{ mg ml}^{-1}$. The temperatures of L - L separation are 285 K at $C_{\text{lys}}=50 \text{ mg ml}^{-1}$ and 287 K at $C_{\text{lys}}=80 \text{ mg ml}^{-1}$ (Ref. 37) and are marked with vertical dashed lines. Symbols represent experimental results from Ref. 22. Lines are results of the model discussed in the text.

model of protein crystallization via an intermediate liquid state. Our goal is a quantitative understanding of the dependence of nucleation on temperature and concentration using parameters that can be measured experimentally.

II. THE MODEL

A. The nucleation rate law

Our main assumption is that in the supersaturated dilute solution a liquidlike cluster is formed with a temperature-dependent and protein-concentration-dependent rate $u_0(C, T)$. This cluster can dissociate back into the solution with rate $u_1(T)$, or it can transform into an ordered crystal nucleus with rate $u_2(T)$. The crystal nucleus irreversibly grows to a macroscopic ordered phase. These processes can be formally described by the following rate scheme:



where state 0 corresponds to the dilute solution, state 1 is the intermediate dense liquid cluster, and state 2 is the final crystalline phase. These three states correspond to the minima in the energy landscape picture in Fig. 2.

The thermodynamic and kinetic parameters of the intermediate and the depth E_1 of the second minimum determine the nucleation rate resulting from this model. For all temperatures above the critical T_c for L - L separation, we assume that the system, via concentration fluctuations, selects the intermediate state leading to fastest nucleation of crystals; $E_1 < E_0$ so that the intermediate is metastable or unstable with respect to the dilute solution. At $T < T_c$, we test two possibilities: (i) state 1 is the same as the dense phase at this temperature; (ii) state 1 is selected according to the same criteria as at $T > T_c$. E_1 becomes greater than E_0 not at T_c but at T_{L-L} at which the chosen dilute solution is in equilibrium with a dense liquid. In all cases, the intermediate has a higher free energy than the final crystalline state.

If we define $P_i(t)$ as a probability to find the system in state $i=0, 1$, or 2 at time t , then a parameter τ

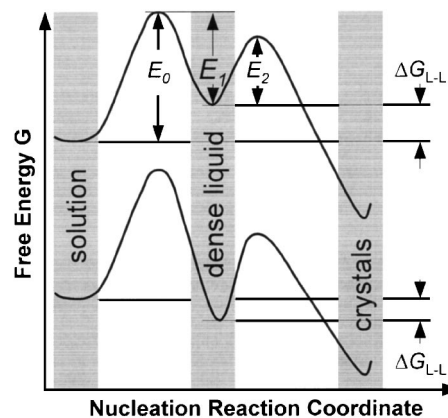


FIG. 2. The free energy G along two possible pathways for nucleation of crystals from solution. E_0 is the barrier for formation of a quasidroplet of dense liquid as a result of a density fluctuation, E_0 is the barrier for decay of these droplets, E_2 the barrier for formation of an ordered cluster as a result of a structure fluctuation within the dense quasidroplet. ΔG_{L-L} is the free energy of formation of the dense liquid phase, $\Delta G_{L-L} > 0$ above the L - L coexistence line and upper curve applies; $\Delta G_{L-L} < 0$ below the L - L coexistence line, reflected by lower curve. See text for discussion of E_1 above the L - L coexistence line.

$= \int_0^\infty t [dP_2(t)/dt] dt$ determines the mean time to create one crystalline nucleus in a steady state process. Thus, the parameter τ represents a mean *first-passage time* for the transition from state 0 to state 2 and is given by³⁴

$$\tau = \frac{1}{u_0(C, T)} + \frac{u_1(T)}{u_0(C, T)u_2(T)} + \frac{1}{u_2(T)}. \quad (2)$$

The rates u_0 , u_1 , and u_2 depend on temperature as $u_i(T) = U_i \exp(-E_i/k_B T)$, $i=0, 1, 2$. As a first simple approximation, the steady-state nucleation rate J can be calculated as $J = \tau^{-1}$. We get for J

$$J = \frac{U_0 U_2 \exp\left(\frac{E_0 + E_2}{k_B T}\right)}{U_0 \exp\left(-\frac{E_0}{k_B T}\right) + U_1 \exp\left(-\frac{E_1}{k_B T}\right) + U_2 \exp\left(-\frac{E_2}{k_B T}\right)}. \quad (3)$$

This is a general expression for the nucleation rate with one intermediate state. Note that it differs significantly from a classical nucleation theory formula with a single temperature-dependent exponent.²⁷

Next, we divide the numerator and denominator on the left side of Eq. (3) by $U_0 \exp(-E_0/k_B T)$, and define a Gibbs free-energy change for the formation of the intermediate $\Delta G = E_0 - E_1$. Since the rate of nucleation of liquid droplets $O(10^7 - 10^9 \text{ cm}^3 \text{ s}^{-1})$ (Ref. 35) is significantly faster than the typical rates of protein crystal nucleation $O(10^{-2} - 1 \text{ cm}^3 \text{ s}^{-1})$,³⁶ we assume that $u_2(T) \ll u_0(T)$, i.e., the structuring of the dense liquid droplets is a rate-limiting step. Equation (3) simplifies to

$$J = \frac{U_2 \exp\left(-\frac{E_2}{k_B T}\right)}{1 + \frac{U_1}{U_0} \exp\left(\frac{\Delta G}{k_B T}\right)}. \quad (4)$$

Equation (4) shows that J does not explicitly depend on the size of the barrier for decay of the dense liquid intermediate: even if $E_1=0$ and the intermediate is unstable (this corresponds to a typical density fluctuation), the expression for J does not change.

B. The maximum in the nucleation rate

Assuming that U_1/U_0 , U_2 , and E_2 are not functions of temperature, we solve the equation $(\partial J/\partial T)_{T^*}=0$ and find that the nucleation rate reaches a maximum at a temperature T^* determined from

$$\frac{E_2}{k_B T^{*2}} \left[1 + \frac{\exp\left(-\frac{\Delta G}{k_B T^*}\right)}{U_1/U_0} \right] = \left| \frac{\partial}{\partial T} \left(\frac{\Delta G}{k_B T} \right) \right|_{T^*}. \quad (5)$$

If ΔG is independent of temperature, this expressions yields a T^* which is not physically meaningful.

For a more realistic description, we allow E_0 and E_1 to change with temperature. We assume that their difference $\Delta G=0$ at T_{L-L} , and $\Delta G/k_B T$ changes linearly with T both above and below T_{L-L} . To find the increment of this dependence, we assume that it equals the temperature increment of the dependence of the free-energy change for $L-L$ separation ΔG_{L-L} below the critical temperature for $L-L$ separation T_c .³⁷ To find this ΔG_{L-L} increment, we use the known strong dependence of enthalpy of $L-L$ separation Δh_{L-L} on temperature that yields $\Delta h_{L-L}=-40$ kJ/mol at $T_c-T \approx 10$ K.³⁷ Integrating numerically the Gibbs-Helmholtz equation with this $\Delta h_{L-L}(T)$, we find that ΔG_{L-L} is an increasing power-law function of T_c-T . Approximating this $\Delta G_{L-L}(T)$ dependence with $\Delta G_{L-L}/k_B T=AT+B$, we get $A=0.0666$. Using the same A for $\Delta G/k_B T$ at T both above and below T_{L-L} , we find that $B=-18.9$ ensures that $\Delta G=0$ at T_{L-L} for $C=50$ mg/ml, while $B=-19.2$ for $C=80$ mg/ml, the two concentrations of the data in Fig. 1. Then, from Eq. (5) with $E_2 \sim k_B T$, $T^* \sim 170$ K, far below that observed experimentally. More importantly, we find (model results not shown) that the nucleation rate J egresses toward the maximum at T^* upon temperature decrease not by a steep exponential as in Fig. 1, but rather by a weak sublinear function.

C. Using the system parameters

The above considerations show that a model that could adequately describe the data in Fig. 1 should account for the physical specificity of the system and of the chosen kinetic model, as well as for the temperature dependence of E_2 .

A crucial element of the model is the nature of the intermediate state. We assume that is akin to the dense liquid and exists at the same temperature as the dilute solution. This allows us use the above linear dependence $\Delta G(T)$ on both sides of T_{L-L} , and this is equivalent to assuming that $E_1 \neq 0$ at $T > T_{L-L}$, i.e., the intermediate is not a mere density fluctuation. The alternative assumption would lead to a break in ΔG at T_{L-L} and a discontinuity in the $J(T)$ dependence. The absence of such discontinuity in Fig. 1 suggests that the intermediate is metastable and has a finite lifetime. Experimental

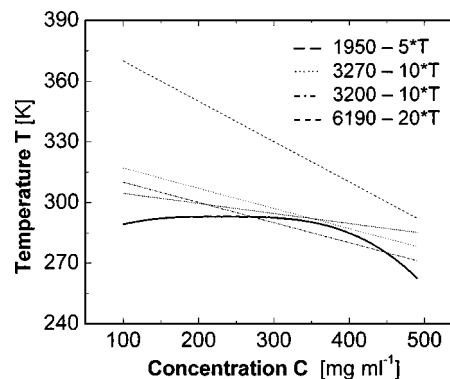


FIG. 3. Assumed value of the concentration of the dense phase intermediate. Dashed, dotted, dash-dotted, and short-dashed lines correspond to different assumptions of this concentration, as indicated in the plot. Solid line marks liquid-liquid coexistence line and is shown for comparison.

evidence of the existence of such a metastable intermediate has now been found for three protein, including lysozyme, data which are modeled here, using dynamic light scattering.³⁸

While these tests show that the size of the metastable liquid droplets is from a few tens to a few hundred nanometers, neither this nor any other technique can provide an estimate of the protein concentration in these droplets. We assume that at each temperature, an intermediate state with a concentration C_1 that does not depend on the dilute solution concentration is selected and that C_1 obeys

$$C_1 = A_1 T + B_1. \quad (6)$$

Below, we show that the nucleation rate law depends only weakly on the exact values of A_1 and B_1 as long as the resulting C_1 in the range $T < T_c$ is in the vicinity of the equilibrium concentration of the dense liquid. The $C_1(T)$ dependencies tested below are depicted in Fig. 3.

The preexponential factor U_2 in Eq. (4) accounts for the kinetics of growth of ordered clusters within the dense liquid droplet, and it should depend on the temperature, concentration, and viscosity within the droplet. In analogy to the preexponential factors for nucleation of solids in melts, we assume that U_2 is proportional to C_1 and T and inversely proportional to viscosity in the dense liquid η at concentration C_1 (Ref. 39),

$$U_2 = k_2 \frac{C_1 T}{\eta(C_1, T)}, \quad (7)$$

where k_2 is a kinetic constant.

We assume that η follows the same dependence in the dilute solution and in the dense liquid and represent $\eta(C, T)$ as the product of the Andrade-Eyring expression for the temperature dependence⁴⁰ and an empirical expression for the concentration dependence.⁴¹ We get

$$\eta = \eta_0 \{1 + [\eta] C_1 \exp(k_\eta [\eta] C_1)\} \exp(-E_\eta/k_B T), \quad (8)$$

where η_0 is the viscosity of the solvent, $[\eta]$ is the viscosity increment at low concentrations, E_η is the Arrhenius-type temperature factor for the viscosity, and k_η is a parameter typically determined by fitting $\eta(C)$ dependencies to Eq. (8); k_η takes values from 1 to 10.⁴¹ The former three parameters

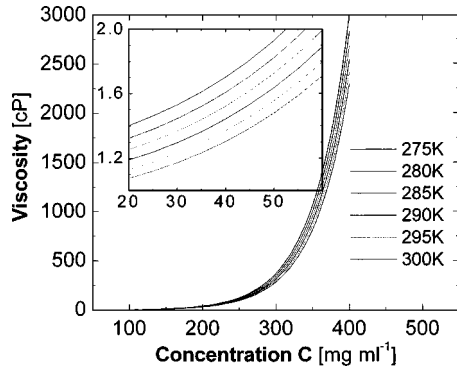


FIG. 4. The dependencies of the viscosity η on protein concentration C_{lys} and temperature T according to Eq. (8) assumed in the model evaluations. The dependencies at low concentrations shown in the inset were fitted to experimental determinations of $\eta(C_{\text{lys}}, T)$ from Ref. 42.

can be determined by fitting Eq. (8) to the data on the viscosity of low-concentration lysozyme solutions at various temperatures.⁴² Thus, in all cases $\eta_0=0.051$ cP, $[\eta]=0.0045$ mg^{-1} ml, and $E_\eta=-7.3$ kJ/mol. The resulting $\eta(C, T)$ curves with $k_\eta=4$ are shown in Fig. 4. As expected, they diverge as C approaches 600 mg ml^{-1} with a corresponding volume fraction 0.49, the noninteracting hard sphere limit.⁴¹

The expression for u_0 in Eq. (4) above is the rate of nucleation of dense liquid droplets and thus the preexponential factor U_0 is a linear function of the dilute solution concentration.^{43,44} Since we know nothing about U_1 we assume that it is constant, so that the ratio $U_1/U_0=1$ for $C=50$ mg ml^{-1} and $50/C$ for other dilute solution concentrations C .

D. The barrier E_2

The steep dependence of J on the deviation of the temperature from the value at solution-crystal equilibrium suggests that the barrier E_2 should be a decreasing function of temperature. Furthermore, comparing the temperatures of the maxima in Fig. 1 at the two studied concentrations to locations in the (C, T) plane, where the nucleus size decreases to one molecule and the nucleation barrier vanishes,^{23,38} we find that they coincide. In analogy to the similar phase locations in phase diagrams of fluids,²⁴⁻²⁶ we assign this temperature to the crystallization spinodal and denote it with T_{sp} . Note that this spinodal is kinetically determined and denotes a location where the solution loses stability with respect to a combination of concentration and structure fluctuations. This

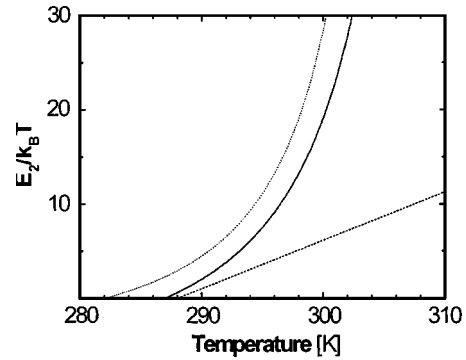


FIG. 5. The dependencies of the barrier E_2 for nucleation of crystals from the dense phase intermediate on temperature T , calculated according to Eq. (9) using solution-crystal equilibrium temperature T_e and crystallization spinodal temperature T_{sp} from Table I, for three of the modeled cases: upper dotted line: 80 mg ml^{-1} lysozyme, 5% glycerol; intermediate solid line: 50 mg ml^{-1} lysozyme; lower dashed line: 80 mg ml^{-1} lysozyme.

differs from the spinodal (or pseudospinodal⁴⁵) for L - L separation introduced in Ref. 37, which may be related to stability loss by concentration fluctuations alone.

We assume that between T_e and T_{sp} , E_2 smoothly decreases from infinity to zero, and in analogy to a recently introduced law,⁴⁶ follows a ΔT^{-2} dependence,

$$E_2(T) = \frac{E^*}{(T_e - T)^2} \left[1 - \frac{(T_e - T)^2}{(T_e - T_{\text{sp}})^2} \right]. \quad (9)$$

The parameter E^* is determined from the following considerations. At T higher than T_{L-L} by several degrees, the nucleation barrier should be $\approx n^* \Delta\mu/2$, where n^* is the nucleus size and $\Delta\mu$ is the thermodynamic supersaturation. Since $\Delta\mu/k_B T \approx 2-3$ and n^* is between 4 and 10,²³ the barrier should be several $k_B T$ units. Using the values of T_e and T_{sp} from Table I and assuming $E^*=15\,000$ kJ mol^{-1} , we get the $E_2(T)$ dependencies shown in Fig. 5, which fulfill this requirement. Note that E^* corresponds to the nucleation barrier E_2 only in the immediate vicinity of T_e , where E_2 approaches infinity. Thus, the high value of E^* allows a strong dependence of E_2 on ΔT via Eq. (9) that results in $E_2 \approx 50$ kJ mol^{-1} at $T=300$ K, where nucleation is still extremely slow, see Fig. 1.

III. MODEL EVALUATION

A. Pure solutions

Lysozyme solutions represent a unique protein system, for which the available data provide values or reasonable estimates for most of the parameters of the above model. The

TABLE I. Thermodynamic characteristics: temperatures of solid-liquid equilibrium T_e , liquid-liquid equilibrium T_{L-L} , and the crystallization spinodal (see text for definition) T_{sp} used in the model calculations, all three from Refs. 22 and 37. The kinetic parameters: kinetic coefficients for viscosity k_η and structuring of intermediate k_2 , and scaling factor for second free-energy barrier E^* used in model calculations. In all cases here, the parameters in the $C_1(T)$ dependence in Eq. (6) are $A_1=-10$ and $B_1=3270$.

	Model characteristics	T_{L-L} (K)	T_{sp} (K)	T_e (K)	k_η	k_2	E^* (kJ/mol)
1	$C=50$ mg ml^{-1}	285	287	315	4	0.266	15 000
2	$C=80$ mg ml^{-1}	287	288	319	4	0.266	15 000
3	$C=50$ mg ml^{-1} , 5% glycerol	278	281	311	4	1.862	10 000
4	$C=50$ mg ml^{-1} , 0.2% PEG	285	287	315	4	0.8911	15 000

TABLE II. Values of the parameters used in model calculations probing the effects of the choice of concentration of intermediate C_1 on the nucleation rate law; thermodynamic characteristics T_{L-L} , T_{sp} , and T_e as in case 1 in Table I.

	Model characteristics	C_1			E^* (kJ/mol)	
		A_1	B_1	k_η		
5	$C=50 \text{ mg ml}^{-1}$ and $C=80 \text{ mg ml}^{-1}$, C_1 follows $T_{L-L}(C)$	-10	3200	7	42.56	15 000
6	$C=50 \text{ mg ml}^{-1}$ and $C=80 \text{ mg ml}^{-1}$	-10	3200	4	0.077	18 000
7	$C=50 \text{ mg ml}^{-1}$ and $C=80 \text{ mg ml}^{-1}$	-5	1950	7.5	1284	15 000
8	$C=50 \text{ mg ml}^{-1}$ and $C=80 \text{ mg ml}^{-1}$	-20	6190	2	0.0114	15 000

only materials parameter missing is k_η , accounting for high-concentration effects in the dependence of the viscosity of the dense liquid intermediate on concentration and temperature in Eq. (8). Thus, k_η remains an adjustable parameter of the model. The other inevitably (due to our low understanding of nucleation in dense liquids) adjustable parameter is the coefficient k_2 in the preexponential factor for the ordering of the dense liquid intermediate U_2 in Eq. (7). Using the values of the respective characteristic temperatures T_e , T_{L-L} , and T_{sp} and the parameters listed in Table I, we fit the model predictions to the data at $C=50 \text{ mg ml}^{-1}$ in Fig. 1. The values of k_2 and k_η yielding the best fit are shown in Table I. Note that all values of k_η are within the range 1–10 found with other solutions for which the viscosity at high concentration has been studied.⁴¹

Using the characteristic temperatures for $C=80 \text{ mg ml}^{-1}$ and the same kinetic parameters as those for $C=50 \text{ mg ml}^{-1}$, we evaluated the model for the former protein concentration. Figure 1 shows that the correspondence between the model prediction and the actual data for $C=80 \text{ mg ml}^{-1}$ is remarkably good.

B. The concentration C_1 in the dense liquid intermediate

To evaluate the significance of the accuracy of the guess of the concentration within the dense liquid intermediate, we evaluated the dependence $J(C_1)$ stemming from Eqs. (4), (7), and (8) at several $T=\text{const}$. We got very shallow maxima at C_1 's near and to the right of the $L-L$ coexistence line. The increase in J to the left of these maxima is due to the dependence in Eq. (7), while the decrease to the right of maxima, to Eq. (8). The shallowness of the maxima indicates that the exact selection of C_1 is not crucial for the resulting value of the nucleation rate. Since the nucleation follows the fastest pathway, we chose the parameters $A_1=-10$ and $B_1=3270$ in Eq. (6) that ensure C_1 values in the region of these maxima.

As a second test of the significance of C_1 , we evaluated the model with different values of the parameters A_1 and B_1 in Eq. (6). If the tested $C_1(T)$ dependence runs near to the case modeled above, such as cases 6 and 7 in Table II and Fig. 3, slight adjustments of the values of the parameters k_η and E^* within their acceptable physical ranges ensure a perfect fit of the model to the experimental results for both $C=50 \text{ mg ml}^{-1}$ and $C=80 \text{ mg ml}^{-1}$.

However, if the tested $C_1(T)$ dependence lay far from case modeled above, such as case 8 in Table II and Fig. 3, the model could not be fit to any of the data sets because of the

high η values in the high-concentration region: compare Figs. 3 and 4. In a special case 5 in Table II, $C_1(T)$ was chosen to cross the $L-L$ coexistence line and the model calculations were carried out assuming that C_1 belongs to that line if the linear dependence lies beneath it. The model yielded a second maximum in the $J(T)$ dependence at T where $C_1(T)$ crosses the $L-L$ coexistence line, which, apparently, is absent in the experimental data in Fig. 1.

This latter strong deviation indicates that the intermediate differs from the macroscopic dense liquid phase. On the other hand, the dependence of $C_1(T)$ was introduced assuming that the intermediate is similar to the dense liquid. These are not necessarily contradictory statements. We note that small clusters of a phase may have different properties than the macroscopic phase itself, as suggested by Gibbs.^{46–48} Thus, it is likely that if the intermediate clusters are allowed to grow, they will become macroscopic dense liquid droplets and the suggestion that the intermediate is similar to the dense liquid phase is still valid.³⁰

C. The effects of glycerol and polyethylene glycol on the nucleation rate

The above model provides a framework for the understanding of the experimentally observed effects of two additives, glycerol and polyethylene glycol 8000 (PEG) on the nucleation kinetics:²² it allows discrimination between the effects of the additives on the solution thermodynamics from those on the nucleation kinetics. The experimental results show that glycerol shifts the temperatures of solution-crystal equilibrium and of $L-L$ coexistence and delays the nucleation rate. The low amount of PEG used, 0.2%, does not affect the phase diagram, however, it leads to significant acceleration of the nucleation rate.²²

The experimental results in the presence of glycerol are compared to the model predictions with three sets of parameters. The dashed line in Fig. 6(a) shows that if the effects of glycerol were limited to the effects on solution thermodynamics, the nucleation rate would have been suppressed very significantly. However, the increase of k_2 necessary to fit the model predictions to the experimental data, see Table I, suggest that glycerol significantly accelerates the kinetics of growth of the ordered clusters within the dense liquid intermediate. Furthermore, the scaling factor for E_2 was reduced by 33% indicating that glycerol leads to lower barriers for the nucleation of the ordered phase.

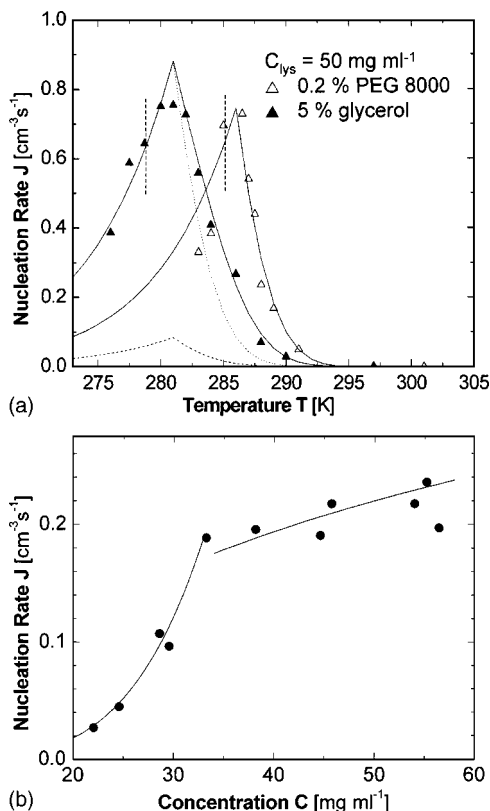


FIG. 6. Additional evaluations of the rate of homogeneous nucleation J of lysozyme crystals. (a) The dependence on temperature T at $C=50 \text{ mg ml}^{-1}$ and in the presence of 5% glycerol or 0.2% polyethylene glycol 8000 as indicated in the plot. Symbols represent experimental results from Ref. 22. Lines are results of the model. For glycerol: dashed line is for T_c and T_{sp} are as in case 3 in Table I, all other parameters are as in case 1 in Table I; dotted line is for T_c and T_{sp} are as in case 3 in Table I, $k_2=1.862$, all other parameters are as in case 1 in Table I; solid line is for all parameters as in case 3 in Table I. For PEG: solid line is for case 4 in Table I. The temperatures of $L-L$ separation are 278 K in the presence of glycerol and 285 K in the presence of PEG, and are marked with vertical dashed lines. (b) The dependence on protein concentration at $T=285.7 \text{ K}$. Symbols represent experimental results from Ref. 23. Lines are results of the model.

The effects of PEG are well modeled by a higher k_2 again suggesting an acceleration of the growth rate of the critical clusters.

We refrain from offering a molecular-level interpretation of the decrease in the barrier for nucleation of ordered clusters within the dense liquid intermediate in the presence of glycerol. However, the accelerated kinetics of growth of the clusters in the presence of both glycerol and PEG is very interesting. We draw an analogy to the \sim ten-fold acceleration of the kinetics of step growth on insulin crystals in the presence of acetone.⁴⁹ This acceleration was attributed to the destruction of the water shells around the insulin molecules in solution by acetone evidenced independently in Ref. 50. The link between the two is the finding that the kinetics of growth of ordered solid phases from solution is limited by the necessity to push structured waters out of the interstice between the incoming molecule and those already in the crystal.³⁷ Glycerol and PEG are similar to acetone in that all three are amphiphilic molecules. Thus, we conclude that the only effect of PEG and the strongest effect of glycerol on the nucleation kinetics occur via the destruction of the water shells of the molecules in the dense liquid precursor.

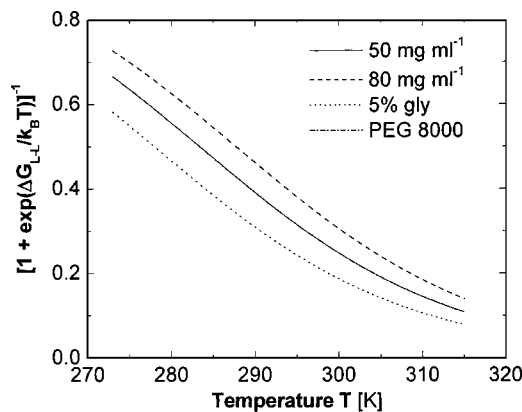


FIG. 7. Evaluation of the contribution of the intermediate to the increase in the nucleation rate at lower temperatures as for the four main model cases as marked in the plot.

D. The dependence of the nucleation rate on protein concentration at constant temperature

The data on $J(C)$ at $T=285.7 \text{ K}$ in Fig. 6(b) is split into two regions. At $C < 33 \text{ mg ml}^{-1}$, J increases quasiexponentially and the nucleus size $n^*=4$ molecules. At $C > 33 \text{ mg ml}^{-1}$, J is a weak function of C and $n^*=1$. In analogy to the spinodal T_{sp} above, we introduce $C_{sp}=33 \text{ mg ml}^{-1}$. To model the dependence $J(C)$, we use the values of ΔG , C_1 , and η at this temperature. We use $U_1/U_0=50/C$ and $E_2=n^*\Delta\mu/2$, with $\Delta\mu=k_B T \ln(C/C_e)$ at $C < C_{sp}$ and $E_2=0$ at $C > C_{sp}$. A good fit of the model results to the experimental data required a slight increase of k_2 from 0.266, see Table I, to 0.2793 at $C < C_{sp}$. Because of the abrupt change of E_2 at C_{sp} , k_2 is needed to be changed to 1.596×10^{-6} for $C > C_{sp}$.

It seems reasonable to assign the necessity of the increase of k_2 at $C < C_{sp}$ to the accumulation of inaccuracies in the values of ΔG , C_1 , and η . Furthermore, the change of k_2 at C_{sp} is due to the jump in the size of the nucleus, reflected in the $J(C)$ data. Such jumps are also a part of the $J(T)$ data in Fig. 1; however, the driving force for the n^* jumps is the decreasing $\Delta\mu$, which is a more sensitive function of T than C . The density of $J(T)$ data points is insufficient to reveal the interruptions in the $n^*(T)$ dependence, and the use of a smooth $E_2(T)$ is appropriate. This smooth $E_2(T)$ allowed the use of a single value of the adjustable parameters k_2 even below T_{sp} . Thus, the good fit of the model results of the data in Fig. 6(b) represent another success of the model.

E. The contribution of the dense liquid intermediate to faster nucleation rates at lower temperatures

As a rough estimate of this contribution, we evaluated the denominator in the nucleation rate law Eq. (4) in Fig. 7; this denominator would not be present in a single step nucleation. Due to our arbitrary choice of U_0 and U_1 , the absolute values of this expression are meaningless. However, we see that as T is lowered, the denominator contributes factors of $\sim 5-7$ in the response of J to T . This contribution enhances at $T > T_{sp}$ the effect of lower E_2 . At $T < T_{sp}$, the acceleration due to lower ΔG is overwhelmed by the deceleration due to higher viscosity within the intermediate.

IV. SUMMARY AND CONCLUSIONS

We have developed a simple phenomenological model describing the kinetics of nucleation of protein ordered solid phases from solution via a metastable intermediate. The model allows accurate predictions of the complex dependencies of the nucleation rate of crystals of the protein lysozyme using a single adjustable kinetic parameter and a reasonable guess of one materials parameter. The good correspondence between the model results and the experimental data supports the following features of the nucleation mechanism.

- (i) The intermediate is similar to the dense liquid existing in lysozyme solutions.
- (ii) The intermediate is metastable with respect to the dilute solution, i.e., a barrier for its decay exists and it is not a simple density fluctuation.
- (iii) The rate-determining step in the nucleation mechanism is the formation of an ordered cluster within the dense liquid intermediate.
- (iv) The viscosity within the metastable dense liquid droplet is a crucial parameter in the kinetics of nucleation of ordered solid phases.

The model allows discrimination between the thermodynamic and kinetic effects of additives that slow down or accelerate nucleation. It suggests that the amphiphilic character of the two tested additives accelerate the kinetics of growth of the near-critical ordered clusters in the dense liquid droplets by destroying the water structures around the protein molecules.

Future theoretical work should address the case of two step nucleation, in which the second step, ordering, is not the rate limiting one. Other potential avenues include understanding of the means to enhance the ordering employed by experimentalists: external fields, shear flow, etc. Experimentalists should provide data on the behavior of protein solution viscosity at high solution concentrations, as well as, of course, data on the nucleation rates with other protein and nonprotein materials.

ACKNOWLEDGMENTS

The authors thank B. Widom and M. E. Fisher for valuable comments. This work was supported by the Office of Biological and Physical Research, NASA (Grant No. NAG8-1854 to P.G.V.), the Camille and Henry Dreyfus New Faculty Award Program (Grant No. NF-00-056 to A.B.K.), the Welch Foundation (Grant No. C-1559 to A.B.K.), and the Alfred P. Sloan Foundation (Grant No. BR-4418 to A.B.K.).

¹S. K. Burley, S. C. Almo, J. B. Bonanno *et al.*, *Nat. Genet.* **23**, 151 (1999).

²K. Wütrich, *Nat. Struct. Biol.* **5**, 492 (1998).

³*Macromolecular Crystallography, Part C*, edited by C. W. Carter, Jr., and R. M. Sweet (Academic, San Diego, 2003), Vol. 368.

⁴W. A. Eaton and J. Hofrichter, in *Advances in Protein Chemistry*, edited by C. B. Anfinsen, J. T. Edsall, F. M. Richards, and D. S. Eisenberg (Academic, San Diego, 1990), Vol. 40, p. 63.

⁵J. W. Kelly, *Nat. Struct. Biol.* **7**, 824 (2000).

⁶M. Bucciattini, E. Giannoni, F. Chiti *et al.*, *Nature (London)* **416**, 507 (2002).

⁷J. Brange, *Galenics of Insulin* (Springer, Berlin, 1987).

⁸P. Reichert, C. McNemar, N. Nagabhushan, T. L. Nagabhushan, S. Tindal, and A. Hruza, U.S. Patent Patent No. 5,441,734 (1995).

⁹A. P. Gast, C. K. Hall, and W. R. Russel, *Faraday Discuss. Chem. Soc.* **76**, 189 (1983).

¹⁰D. F. Rosenbaum, A. Kulkarni, S. Ramakrishnan, and C. F. Zukoski, *J. Chem. Phys.* **111**, 9882 (1999).

¹¹D. F. Rosenbaum, P. C. Zamora, and C. F. Zukoski, *Phys. Rev. Lett.* **76**, 150 (1996).

¹²D. Leckband and J. Israelachvili, *Q. Rev. Biophys.* **34**, 105 (2001).

¹³D. N. Petsev and P. G. Vekilov, *Phys. Rev. Lett.* **84**, 1339 (2000).

¹⁴P. G. Vekilov and A. A. Chernov, in *Solid State Physics*, edited by H. Ehrenreich and F. Spaepen (Academic, New York, 2002), Vol. 57, p. 1.

¹⁵N. Asherie, A. Lomakin, and G. B. Benedek, *Phys. Rev. Lett.* **77**, 4832 (1996).

¹⁶M. Hagen, E. Meijer, G. Mooij, D. Frenkel, and H. Lekkerkerker, *Nature (London)* **365**, 425 (1993).

¹⁷J. A. Thomson, P. Schurtenberger, G. M. Thurston, and G. B. Benedek, *Proc. Natl. Acad. Sci. U.S.A.* **84**, 7079 (1987).

¹⁸C. Liu, N. Asherie, A. Lomakin, J. Pande, O. Ogun, and G. B. Benedek, *Proc. Natl. Acad. Sci. U.S.A.* **93**, 377 (1996).

¹⁹M. Muschol and F. Rosenberger, *J. Chem. Phys.* **107**, 1953 (1997).

²⁰O. Galkin, K. Chen, R. L. Nagel, R. E. Hirsch, and P. G. Vekilov, *Proc. Natl. Acad. Sci. U.S.A.* **99**, 8479 (2002).

²¹Q. Chen, P. G. Vekilov, R. L. Nagel, and R. E. Hirsch, *Biophys. J.* **86**, 1702 (2004).

²²O. Galkin and P. G. Vekilov, *Proc. Natl. Acad. Sci. U.S.A.* **97**, 6277 (2000).

²³O. Galkin and P. G. Vekilov, *J. Am. Chem. Soc.* **122**, 156 (2000).

²⁴J. D. van der Waals, *Nobel Lectures, Physics 1901-1921* (Elsevier, Amsterdam, 1979).

²⁵J. W. Cahn and J. E. Hilliard, *J. Chem. Phys.* **28**, 258 (1958).

²⁶K. Binder and P. Fratzl, in *Phase Transformation in Materials*, edited by G. Kostorz (Wiley, New York, 2001).

²⁷D. Kashchiev, *Nucleation. Basic Theory with Applications* (Butterworth, Oxford, 1999).

²⁸P. R. ten Wolde and D. Frenkel, *Science* **277**, 1975 (1997).

²⁹V. Talanquer and D. W. Oxtoby, *J. Chem. Phys.* **109**, 223 (1998).

³⁰P. G. Vekilov, *Cryst. Growth Des.* **4**, 671 (2004).

³¹V. J. Anderson and H. N. W. Lekkerkerker, *Nature (London)* **416**, 811 (2002).

³²G. Nicolis and C. Nicolis, *Physica A* **323**, 139 (2003).

³³A. Lomakin, N. Asherie, and G. B. Benedek, *Proc. Natl. Acad. Sci. U.S.A.* **100**, 10254 (2003).

³⁴N. G. van Kampen, *Stochastic Processes in Physics and Chemistry* (Elsevier, New York, 1992), Chapt. XII.

³⁵M. Shah, O. Galkin, and P. G. Vekilov, *J. Chem. Phys.* (in press).

³⁶O. Galkin and P. G. Vekilov, *J. Mol. Biol.* **336**, 43 (2004).

³⁷D. N. Petsev, X. Wu, O. Galkin, and P. G. Vekilov, *J. Phys. Chem. B* **107**, 3921 (2003).

³⁸O. Gliko and L. Filobelo (unpublished).

³⁹I. Gutzow and J. Schmelzer, *The Vitreous State* (Springer, Berlin, 1995).

⁴⁰R. B. Bird, W. E. Stewart, and E. N. Lightfoot, *Transport Phenomena* (Wiley, New York, 1960).

⁴¹C. W. Macosco, *Rheology Principles, Measurements and Applications* (VCH, New York, 1994).

⁴²W. J. Fredericks, M. C. Hammonds, S. B. Howard, and F. Rosenberger, *J. Cryst. Growth* **141**, 183 (1994).

⁴³D. Kashchiev, in *Science and Technology of Crystal Growth*, edited by J. P. v. d. Eerden and O. S. L. Bruinsma (Kluwer Academic, Dordrecht, 1995), p. 53.

⁴⁴B. Mutaftshiev, in *Handbook of crystal growth*, edited by D. T. J. Hurle (Elsevier, Amsterdam, 1993), Vol. I, p. 189.

⁴⁵P. G. Debenedetti, *Metastable Liquids* (Princeton University Press, Princeton, 1996).

⁴⁶D. Kashchiev, *J. Chem. Phys.* **118**, 1837 (2003).

⁴⁷J. W. Gibbs, *Trans. Conn. Acad. Arts Sci.* **3**, 108 (1876).

⁴⁸J. W. Gibbs, *Trans. Conn. Acad. Arts Sci.* **16**, 343 (1878).

⁴⁹I. Reviakine, D. K. Georgiou, and P. G. Vekilov, *J. Am. Chem. Soc.* **125**, 11684 (2003).

⁵⁰L. Bergeron, L. Filobelo, O. Galkin, and P. G. Vekilov, *Biophys. J.* **85**, 3935 (2003).